

Photoemission Studies of the Electronic Structure of Cobalt*

A. Y.-C. YU† AND W. E. SPICER

Stanford Electronics Laboratories, Stanford University, Stanford, California

(Received 19 October 1967)

Photoemission measurements have been made on cobalt to study major features of its electronic structure over a large energy range. In the spectral range studied ($7.4 \text{ eV} \leq h\nu \leq 11.6 \text{ eV}$), nondirect transitions dominate. The optical density of states is determined from the photoemission and optical data. Peaks are found in the valence-band structure at about 0.3, 2.4, and 5.2 eV below the Fermi level, and no structure is found in the conduction band for $4.5 \text{ eV} \leq E - E_F \leq 11.5 \text{ eV}$. The $\omega\sigma$ curve is fitted reasonably well using the optical density of states and assuming nondirect transitions. A strong similarity is found between the optical density of filled states for Co and that of Ni and Fe. Thus the optical density of states for Fe, Co, and Ni do not seem to be related via the rigid-band model. A discussion is given on these data and their relevance to other related results.

I. INTRODUCTION

INFORMATION concerning the electronic structure of metals over a wide energy range (about 10 eV below and above the Fermi level) can be provided by photoemission and optical-reflectivity data.¹ Such information has been obtained for Ni² and Fe.³ This is of particular interest because of the occurrence of the ferromagnetism of the 3*d* transition metals. Cobalt was chosen for similar studies because this would complete the 3*d* ferromagnetic series.⁴ In the preceding paper,⁵ the optical-reflectivity studies of Co have been presented and optical functions deduced. In this paper, we shall present and discuss photoemission results of Co samples prepared and studied in high vacuum. The optical density of states⁶ of Co will be determined from the photoemission and optical data, and these results will be discussed and related to other experimental and theoretical data.

II. EXPERIMENTAL METHODS

Photoemission measurements were made on high-vacuum evaporated Co samples in a continuously pumped (oil-free VacIon system) stainless-steel chamber (pressure during measurements was about 5×10^{-9} Torr).⁷ Two types of evaporators were used: W evaporator and electron-gun evaporator. The W evaporator was formed by wrapping 10-mil W wire on 10-mil Co

wire so that the weight of Co is kept below 30% of that of W to avoid alloying.⁸ In the electron-gun evaporator (manufactured by Varian Associates), the evaporant, placed on a water-cooled crucible, was evaporated by electron-beam bombardment. The electron-gun evaporator is superior to the W evaporator for at least two reasons. First, the hot filament was shielded from the crucible so that the evaporant could not be contaminated. Second, the crucible was sufficiently cooled so that it could not unite and alloy with the evaporant. Photoemission results from samples formed by these two types of evaporators were almost identical.⁹ Figures 1 to 3 indicate the reproducibility of the results from various samples. In Fig. 1, the photoemitted-electron-energy-distribution curves (EDC's) at $h\nu = 10.2 \text{ eV}$ of samples prepared by electron-gun and W evaporators are compared.¹⁰ It is clear that the EDC's of these two differently prepared samples have almost exactly the same structure.¹¹ Several samples formed by electron-gun evaporation (pressure during evaporation $\sim 7 \times 10^{-8}$ Torr) were studied, and the results were completely reproducible. Figure 2 compares the EDC's at $h\nu = 10.2 \text{ eV}$ of two electron-gun-evaporated samples (arbitrarily normalized at $E = 3 \text{ eV}$). They are practically identical. At other photon energies, the EDC's are similarly reproducible. The quantum yields of the two electron-gun-evaporated samples are also practically identical (see Fig. 3). Since the structure in the EDC's of the

* W. C. Roberts and T. A. Vanderslice, *Ultrahigh Vacuum and its Applications* (Prentice-Hall Inc., Englewood Cliffs, N. J., 1963), p. 138.

⁹ Note that the structure in the EDC's of Ni films evaporated from Ni-plated W evaporators (Ref. 2) and Ni cleaned by sputtering [W. M. Breen, F. Wooten, and T. Huen, *Phys. Rev.* **159**, 475 (1967)] are also almost identical and independent of sample-preparation methods.

¹⁰ The zero of energy refers to zero bias between collector and emitter of the photodiode. The collector (coated with Cu) has a work function of 4.5 eV.

¹¹ The only significant difference in the EDC's is not due to a difference in the excitation structure but to a variation of work function. Note that the low-energy cutoff of the sample evaporated from W is less sharp and extends to lower energy than the electron-gun-evaporated sample. This indicates a variation of work function across the surface of the W-evaporated sample, with some of "patches" having slightly smaller ($\Delta\phi \cong 0.5 \text{ eV}$) work function than the electron-gun-evaporated samples. This probably is because of the presence of different crystallographic faces. The low-energy cutoff of the electron-gun-evaporated samples is much sharper (see Fig. 2).

* Work supported by the Advanced Research Projects Agency through the Center for Materials Research at Stanford University and by the National Science Foundation.

† Present address: Fairchild Semiconductor Research and Development Laboratory, Palo Alto, Calif.

¹ W. E. Spicer, *Optical Properties and Electronic Structure of Metals and Alloys* (North-Holland Publishing Co., Amsterdam, 1966), p. 296.

² A. J. Blodgett, Jr., and W. E. Spicer, *Phys. Rev.* **146**, 390 (1966).

³ A. J. Blodgett, Jr., and W. E. Spicer, *Phys. Rev.* **158**, 514 (1967).

⁴ A. Y.-C. Yu and W. E. Spicer, *Phys. Rev. Letters* **17**, 1171 (1966).

⁵ A. Y.-C. Yu, T. M. Donovan, and W. E. Spicer, preceding paper, *Phys. Rev.* **167**, 670 (1968).

⁶ The density of states appropriate for optical data (photoemission and reflectivity data) is called the optical density of states. See W. E. Spicer, *Phys. Rev.* **154**, 385 (1967).

⁷ A. Y.-C. Yu, Ph.D. dissertation, Stanford University, 1967 (unpublished).

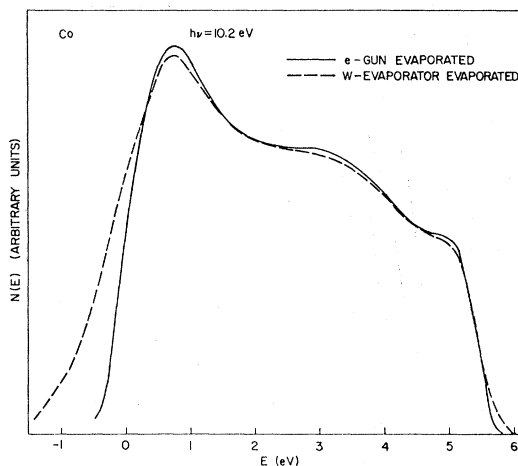


FIG. 1. Comparison of EDC's at $h\nu = 10.2$ eV for samples prepared by two different types of evaporations.

electron-gun-evaporated samples are sharper and completely reproducible, results from one such sample will be presented in Sec. IV.

Techniques for making photoemission measurements (quantum yield and photoemitted-electron-energy distribution) have been reported elsewhere¹² and shall not be discussed here.

III. METHOD OF ANALYSIS OF THE PHOTOEMISSION DATA

When nondirect transitions dominate the optical transitions (such is the case for Co, as will be shown later), the normalized energy-distribution curve (NEDC)¹³ of primary photoemitted electrons (electrons that have not suffered inelastic scattering producing significant energy loss) is given by^{2,14}

$$N(E, h\nu) = CP(E)N_V(E - h\nu)/\omega\sigma, \quad (1)$$

where

$$P(E) = T(E)\alpha L(E)/[1 + \alpha L(E)]M^2 N_C(E), \quad (2)$$

$$\sigma = C/\omega \int_{E_f}^{E_f + h\nu} M^2 N_C(E) N_V(E - h\nu) dE, \quad (3)$$

where

$$C = 8\pi^2 e^2 / 3m^2, \quad (4)$$

$T(E)$ is the threshold function,¹⁵ M^2 is the matrix element squared; $L(E)$ is the attenuation length of photoemitted electrons,¹⁴ and N_V , N_C are the valence-band and conduction-band optical densities of states,⁶

¹² W. E. Spicer and C. N. Berglund, Rev. Sci. Instr. 35, 1665 (1964).

¹³ The area of each NEDC is equal to the quantum yield at the same incident photon energy.

¹⁴ C. N. Berglund and W. E. Spicer, Phys. Rev. 136, A1030 (1964); 136, A1044 (1964).

¹⁵ The threshold function gives the probability for an electron to escape into the vacuum as a function of its kinetic energy.

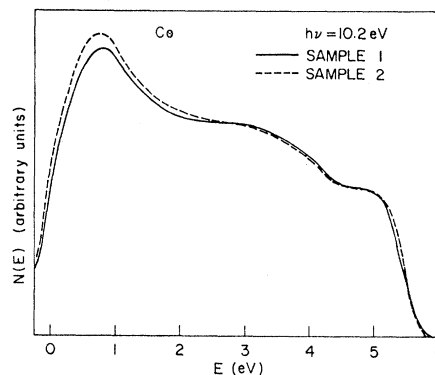


FIG. 2. Photoemitted electron EDC's of two Co samples at $h\nu = 10.2$ eV (arbitrarily normalized at $E = 3$ eV). Both samples were prepared by electron e -gun evaporations.

respectively.¹⁶ $P(E)$ is a function of E only, because α is almost a constant in the spectral range $h\nu = 7$ to 12 eV, as shown in Fig. 8 of the preceding paper.⁵ Note that in Eq. (1), $P(E)$ depends on E and $N_V(E - h\nu)$ on $(E - h\nu)$. Making use of this, it is possible to determine N_V and P from the experimental data. Using the experimental NEDC's (EDC's normalized to yield) and experimental σ , $N_V(E)$ and $P(E)$ can be determined from Eqs. (1) and (2), assuming M^2 to be a constant.^{2,14} A self-consistent test can then be made by calculating

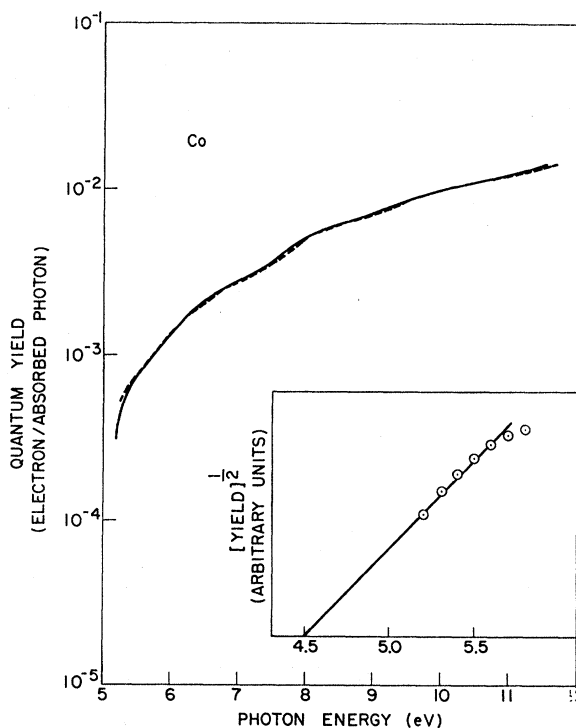


FIG. 3. Quantum-yield and work-function determination of Co.

¹⁶ Although Eq. (1) only includes primary electrons, it is a good approximation, since the fraction of photoemitted electrons which escape after electron-electron scattering is usually small if the work function is high (~ 5 eV) and $h\nu$ is sufficiently low ($h\nu < 12$ eV). These conditions are met for Co.

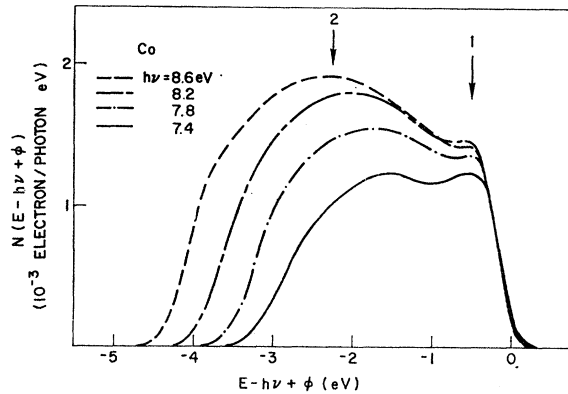


FIG. 4. EDC's of Co for $7.4 \text{ eV} \leq h\nu \leq 8.6 \text{ eV}$, plotted versus $E-h\nu+\phi$.

all of the NEDC's from the N_V and P so determined. Note that since normalized EDC's are used, the test is for magnitude as well as for shape of the NEDC's.¹⁷

Structure in the conduction band above the vacuum level can be identified from EDC's since they are stationary in energy, as can be seen from Eqs. (1) and (2). Conduction-band states below the vacuum level cannot be revealed by photoemission, although they can be indirectly obtained by a comparison between experimental σ and σ calculated from the N_V determined from photoemission and by using different assumed N_G . The detailed procedure for deducing the optical density of states of Co will be presented in Sec. V. In addition to the optical density of states, it is possible to obtain information about $L(E)$ and/or $T(E)$ from $P(E)$. This will be discussed in Appendix A.

IV. PHOTOEMISSION RESULTS

A. Quantum Yield

The quantum yield of Co (sample 1) is presented in Fig. 3. The yield is quite low, rising to only about 0.014

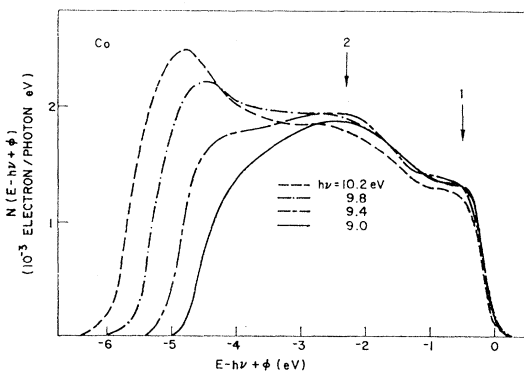


FIG. 5. EDC's of Co for $9.0 \text{ eV} \leq h\nu \leq 10.2 \text{ eV}$, plotted versus $E-h\nu+\phi$.

¹⁷ Note that in the earlier work of Blodgett and Spicer (Refs. 2 and 3), the fit was only relative. Thus an added constraint has been put on the analysis of the experimental data in the present work. This improvement in the analysis results from increased accuracy in the absolute calibration of the quantum yield.

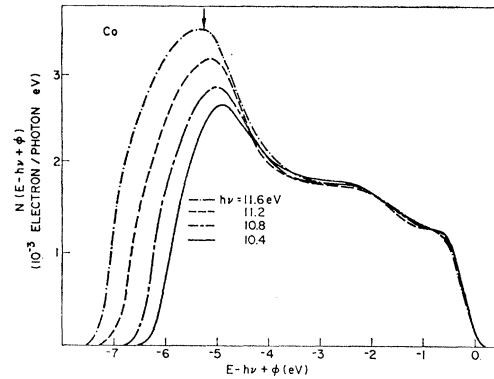


FIG. 6. EDC's of Co for $10.4 \text{ eV} \leq h\nu \leq 11.6 \text{ eV}$, plotted versus $E-h\nu+\phi$.

electrons per absorbed photon at $h\nu=11.5 \text{ eV}$. The yield curve is smooth and lacking of strong structure. The work function of this sample has been determined to be 4.5 eV by the Fowler plot (Fig. 3), in reasonable agreement with those found by Suhrman and Wedler¹⁸ (4.6 eV) and Samsonov¹⁹ (4.41 eV).

B. Photoemitted-Electron-Energy Distributions

It can be seen from Eq. (1) that if the EDC's are plotted versus $(E-h\nu)+\phi$ (i.e., if the EDC's are referred to the energy associated with the valence-state hole created by the excitation), structure due to the valence band will superimpose. In Figs. 4 to 6, NEDC's (energy-distribution curves normalized to yield) are presented. In Fig. 4 ($7.4 \text{ eV} \leq h\nu \leq 8.6 \text{ eV}$), one peak (indicated by arrow 1) superimposes, and another peak (under arrow 2) starts to be exposed. In Fig. 5, NEDC's for $9.0 \text{ eV} \leq h\nu \leq 10.2 \text{ eV}$ are shown. For these curves, two pieces of structure (under arrows 1 and 2) superimpose very well. Beginning with $h\nu \leq 9.8 \text{ eV}$, a third piece of structure starts to be exposed. For higher photon energies (Fig. 6), this third structure (under arrow) almost superimposes. Because of the LiF window (cutoff at about $h\nu=11.8 \text{ eV}$), EDC's with higher photon energies cannot be measured. In Fig. 7, the EDC's for $h\nu=10.4$ to 11.6 eV are plotted versus the electron kinetic energy in the vacuum.²⁰ It is clear that the low-energy peak (arrowed) is moving out with photon energy. Experience¹⁴ indicates that a peak of scattered electrons due to ordinary electron-electron scattering as previously treated will be stationary in energy in the EDC's. It may be tempting to attribute this low-energy peak in the EDC's to electrons suffering discrete loss subsequent to the optical excitation. This seems unlikely, since the energy-loss spectra of Co²¹

¹⁸ V. R. Suhrman and G. Wedler, *Z. Angew. Phys.* **14**, 70 (1962).

¹⁹ *Handbook of Thermionic Properties*, edited by G. V. Samsonov (Plenum Press, Inc., New York, 1966).

²⁰ All the EDC's have tails extending to below zero because of a large ac voltage used and slight nonuniformity of the sample work function.

²¹ J. L. Robins and J. B. Swan, *Proc. Phys. Soc. (London)* **76**, 857 (1960).

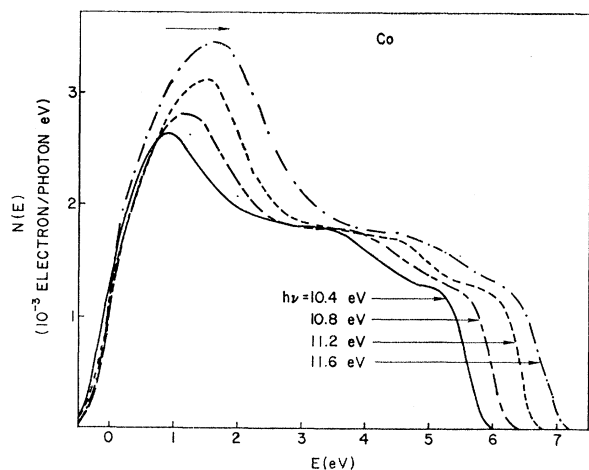


FIG. 7. EDC's of Co for $10.4 \text{ eV} \leq h\nu \leq 11.6 \text{ eV}$, plotted versus E .

has only a very weak shoulder at about 4.6 eV. Furthermore, it is difficult to explain the peak in $\omega\sigma$ at $h\nu = 6 \text{ eV}$ in this picture. As we shall see later, the 6-eV peak in $\omega\sigma$ can be very simply explained by our nondirect-transition model.

In Fig. 6, it is clear that three pieces of structure superimpose at $E - h\nu + \varphi = -0.6, -2.4,$ and -5.2 eV . This superposition of structure over a wide spectral range ($7.4 \text{ eV} \leq h\nu \leq 11.6 \text{ eV}$) indicates that nondirect transitions do dominate there and that it should bear a close resemblance to the valence-band optical density of states.²² It has been suggested that this peak which moves out is not due to the conventional electron-electron scattering, but to a discrete scattering mechanism. In order to place this suggestion in perspective, we will return to it in Sec. V after determining the optical density of states.

When one compares the EDC's of Co with those of Ni, they are found to be very similar. A representative comparison is shown in Fig. 8, with photon energy 10.2 eV (arbitrarily normalized at $E = 5 \text{ eV}$). The only

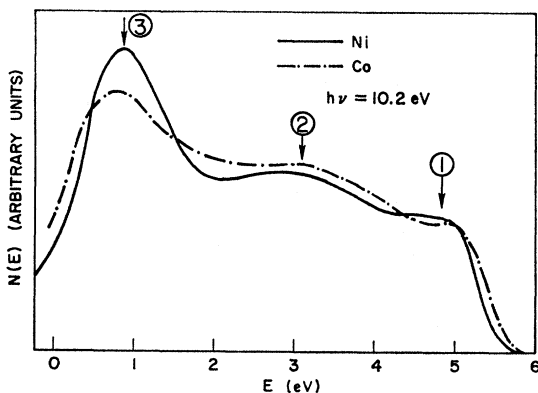


FIG. 8. Comparison of EDC's of Ni and Co at $h\nu = 10.2 \text{ eV}$.

²² This is because $P(E)$ lacks any structure, as can be seen from Fig. 10.

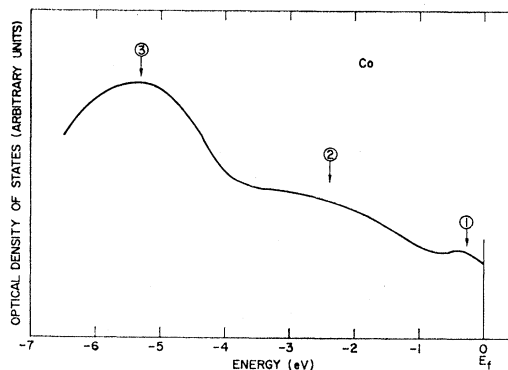


FIG. 9. Valence-band optical density of states of Co.

appreciable difference is that the peak in Ni at $E = 0.8 \text{ eV}$ is relatively higher than that of Co. This suggests that the low-energy peak in the optical density of states of Ni at $E - E_f = 4.6 \text{ eV}$ is relatively higher than that of Co.

To summarize, the optical transitions in the spectral range $7.4 \text{ eV} \leq h\nu \leq 11.6 \text{ eV}$ are found to be predominantly nondirect from examining the EDC's. The structure in the EDC's superimposes on an $E - h\nu + \varphi$ plot, indicating that it is due to the valence-band optical density of states. The EDC's of Co are also found to be strikingly similar to those of Ni, though the low-energy peak is somewhat lower than that of Ni.

V. DETERMINATION OF THE OPTICAL DENSITY OF STATES

A. Valence-Band Optical Density of States $N_V(E)$ and $P(E)$

Since the optical transitions are found to be nondirect in the spectral range studied, the optical density of states can be obtained from the photoemission data as described in Sec. III. The $N_V(E)$ and $P(E)$ as deduced from the NEDC's using Eq. (1) are shown in Figs. 9 and 10, respectively. A self-consistency check can be made by using $P(E)$ and $N_V(E)$ to calculate NEDC's for the complete range of $h\nu$.

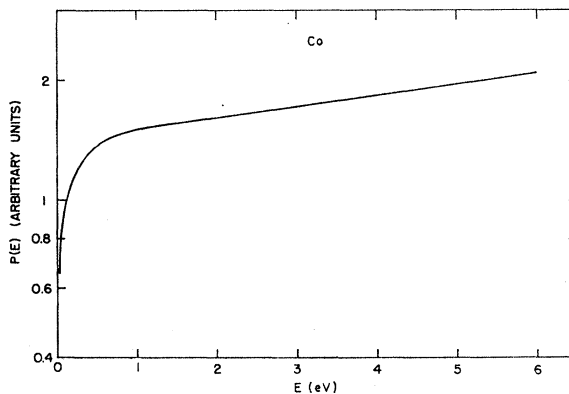


FIG. 10. Plot of $P(E)$ of Co.

In Fig. 11, the calculated and experimental primary-electron EDC's are compared. The agreement is relatively good in both shape and magnitude. These curves are displaced vertically for clarity. The good absolute agreement between the calculated and measured NEDC's (for most of the curves the agreement is within $\pm 5\%$) indicates that the nondirect-transition

model with constant matrix is applicable and that photoemitted-electron EDC's are well described by Eq. (1). Note that the experimental quantum yield includes electrons that had suffered electron-electron scattering within the solid as well as primary electrons, though the former is only a small fraction ($\sim 10\text{--}25\%$). The fraction of scattered electrons in the experimental

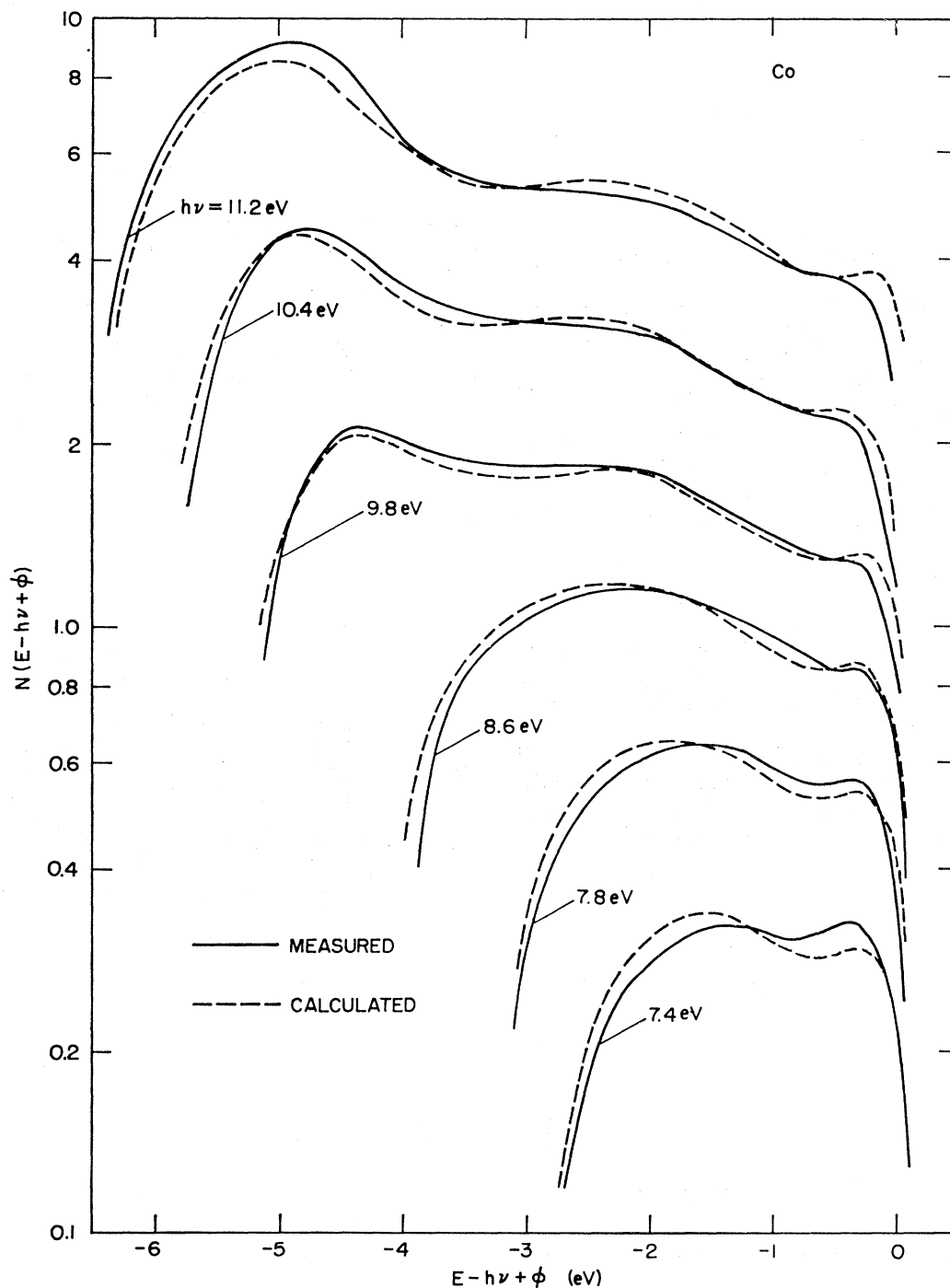
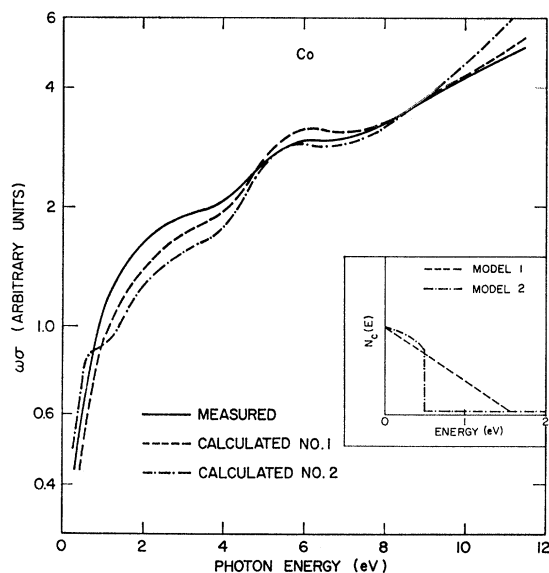


FIG. 11. Comparison of measured and calculated EDC's.

FIG. 12. Calculation of $\omega\sigma$.

yield can be estimated from a constant-optical-density-of-states model²³ and subtracted. The experimental EDC's are then normalized to the corrected yield, which only includes primary electrons.

B. Conduction-Band Optical Density of States $N_C(E)$

N_V and P have been determined. N_C is then chosen so that the calculated $\omega\sigma$ ($=\omega^2\epsilon_2$) (assuming M^2 is a constant) agrees with experiment. It is expected that N_C joins continuously with N_V at the Fermi level and decreases for higher energies, similar to that of Ni. In Fig. 12, two different N_C 's (they are identical for $E-E_f \geq 2$ eV) and the calculated $\omega\sigma$'s are shown (with the same N_V as in Fig. 9), along with the measured $\omega\sigma$. The No. 2 N_C has the same form as that of Ni.² However, the agreement between the measured and calculated $\omega\sigma$ and this N_C is not very satisfactory. The No. 1 N_C yields $\omega\sigma$, in good agreement with experiment. It is clear from Fig. 12 that the shape of $\omega\sigma$ in the infrared and visible depends critically on the N_C near the Fermi surface, while $\omega\sigma$ at higher photon energies is not so sensitive. Note that only the shape of $\omega\sigma$ is calculated. The magnitude has been adjusted to fit experiment. It should be pointed out that in order to have agreement between the calculated and the measured $\omega\sigma$ for $h\nu > 6$ eV, it is necessary to have the conduction-band optical density of states increase slowly with energy for $E-E_f \geq 6$ eV, as shown in Fig. 13.

Our best calculated $\omega\sigma$ is noticeably lower than that measured around $h\nu=2-3$ eV. Within the constraints of our model, we were not able to adjust N_C to produce

²³ A. J. Blodgett, Jr., Ph.D. dissertation, Stanford University, 1965, p. 17 (unpublished). Using the constant-optical-density model, there are approximately 21% scattered electrons at $h\nu=11.2$ eV and 11% at $h\nu=7.8$ eV for Co.

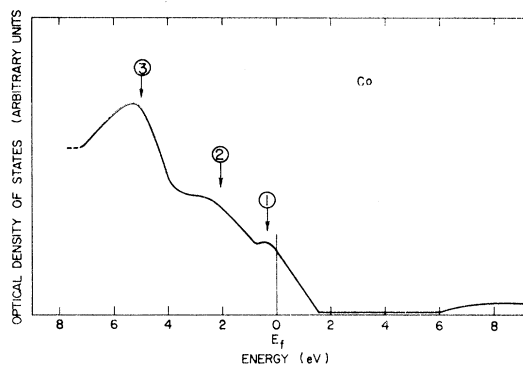


FIG. 13. The complete optical density of states of Co.

a better agreement. The discrepancy is probably due to matrix-element variation there. Note that α shows a peak at $h\nu=3$ eV (Fig. 8 of the preceding paper³), and this cannot be explained by our constant-matrix-element model with the optical density of states in Fig. 13.

It should be pointed out that in our model, the peak in $\omega\sigma$ at $h\nu=6$ eV (or the peak in α at $h\nu=6$ and ϵ_2 at $h\nu=5.5$ eV) is due to transitions from the strong valence-band-optical-density-of-states peak at $E-E_f=-5.2$ eV to the empty states just above the Fermi level. Thus this strong peak in the valence band is essential in explaining the optical as well as the photoemission data.

In Fig. 13, the complete optical density of states of Co is shown. The optical density of states of Co is very similar to that of Ni² and Fe.³ In Fig. 14, they are compared. The three curves have been arbitrarily normalized at -2.5 eV. For -3 eV $\leq E-E_f \leq 0$, they are very similar, with a small peak at about $E-E_f=-0.3$ eV and a broad peak at about $E-E_f=-2.4$ eV. There is a peak in Ni at $E-E_f=-4.6$ eV and in Fe at $E-E_f=-5.5$ eV not anticipated by the older band calculations. A similar peak is also present in Co at $E-E_f=-5.2$ eV, with height intermediate between that of Ni and Fe. The peak positions of these three metals are summarized in Table I. The similarity of the optical densities of states of these metals is striking, since they all have different crystal structures [Ni (fcc), Co (hcp), and Fe (bcc)]. It suggests that the crystal symmetry does not have a first-order effect on the optical density of states.

C. Discussion of Co Optical Density of States

The valence band of Co has nine electrons. This would fix the absolute scale on the vertical axis of the optical density of states if we put nine electrons in states -7 eV $\leq E-E_f \leq 0$ (note that the band is cut off at $E-E_f=-7$ eV). The optical density of states at the Fermi level is found to be 0.56 electron/atom eV, compared with the specific-heat density

TABLE I. Position of structures in the optical densities of states of Ni, Co, and Fe.

Metal	Peak 1 (eV)	Peak 2 (eV)	Peak 3 (eV)
Ni	-0.3 ± 0.1	-2.2 ± 0.2	-4.6 ± 0.1
Co	-0.3 ± 0.1	-2.4 ± 0.2	-5.2 ± 0.2
Fe	-0.35 ± 0.1	-2.4 ± 0.2	-5.5 ± 0.2

of states of 2.12 electron/atom eV.²⁴ This discrepancy may be due to large electron-phonon interaction^{25,26} or other many-body effects. The conduction-band optical density of states for $0 \leq E - E_f \leq 1.5$ eV corresponds to only 0.45 electrons instead of 1.72 electrons (saturation magnetic moment of Co of $1.72 \mu_B/\text{atom}$ ²⁷). This may be due to the fact that when we calculate $\omega\sigma$ by Eq. (3), we have assumed M^2 to be a constant and lumped that into N_C .²⁸

There is one type of matrix-element variation which would go undetected in the photoemission and optical studies.²⁹ In Eq. (1) to (3), the matrix element was treated as a constant; however, if valence states at a given energy E_1 were coupled more strongly to all final states than were initial states at all other energies, a corresponding increase would appear in the initial optical density of states. Watson³⁰ and Freeman³¹ have pointed out that such effects might account for much of the deep peak in Co, Ni, Fe, and Cu. We will discuss this point in detail in the next section.

VI. DISCUSSION AND CONCLUSIONS

The valence-band optical densities of states of the three ferromagnetic transition metals Fe,³ Co, and Ni² are presented in Fig. 14. The similarity between the three curves is striking. The peaks labeled 1 and 2 coincide almost exactly, and all contain the deep peak labeled 3. Before commenting further on the similarity between these materials, it is important to emphasize the value of comparing the optical densities of states of related materials.

As has been pointed out previously,²⁹ it is not yet clear how closely the optical density of states resembles the unperturbed ground-state density of states for a

²⁴ F. E. Hoare, *Electronic Structure and Alloy Chemistry of the Transition Elements* (Interscience Publishers, Inc., New York, 1963), p. 35.

²⁵ A. M. Clogston, *Phys. Rev.* **136**, A8 (1964).

²⁶ K. Kerbs, *Phys. Letters* **6**, 31 (1963).

²⁷ C. Kittel, *Introduction to Solid State Physics* (John Wiley & Sons, Inc., New York, 1956), 2nd ed., p. 407.

²⁸ Note that Blodgett and Spicer (Ref. 2) obtained 0.45 d holes for Ni from the optical density of states, in reasonable agreement with the saturation magnetization of $0.6 \mu_B/\text{atom}$ of Ni. As indicated in Ref. 17, we have refined our analysis to have good agreement between the calculated and measured EDC's in both shapes and magnitudes. Such a refinement in the analysis of the Ni data should increase the strength of the peak at $E - E_f = 4.6$ eV and reduce the number of d holes.

²⁹ W. E. Spicer, *Phys. Rev.* **154**, 385 (1967).

³⁰ J. R. Cuthill, A. J. McAlister, M. L. Williams, and R. E. Watson, *Phys. Rev.* **164**, 1006 (1967); and (private communication).

³¹ A. J. Freeman (private communication).

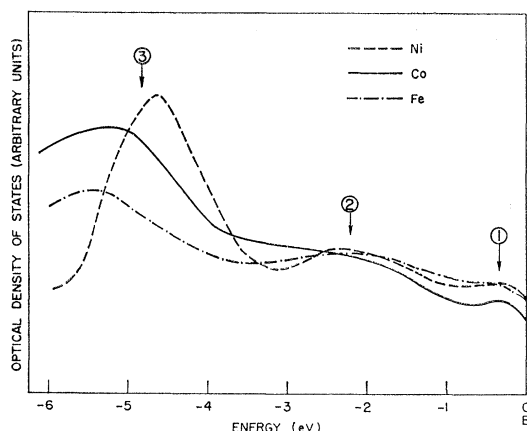


FIG. 14. Comparison of the optical densities of states of Ni, Co, and Fe.

given material. There may be a close relationship between these two densities of states if two conditions are satisfied: (1) The interaction(s) through which the \bar{k} of the total system is conserved must not siphon appreciable energy from the primary electron-hole excitation (e.g., an indirect excitation involving the creation of a photon would not siphon off an appreciable amount of energy), and (2) there must be no important matrix-element modulation for transitions for a given initial state to all final states.³² However, if the two conditions cited above do not hold, important differences could occur between the two densities of states. We suggest here that the possible problems inherent in relating these two densities of states can be at least partially eliminated by comparing the optical densities of closely related materials. Systematic similarities or differences should reflect similarities or differences in the electronic structure and/or the many-body interaction in the materials compared. Here we will compare the optical densities of states of three ferromagnetic transition elements and also comment on their relation to Cu and Pd. A discussion will also be given of relationships between the present results and the results of band calculations, as well as the results obtained using different experimental techniques.

Return now to Fig. 14 and the comparison of the optical densities of states of Fe, Co, and Ni. The curves are quite similar. The peaks labeled 1, 2, and 3 almost coincide.³³ This similarity is particularly striking, since the three materials all have different crystal structures [Ni (fcc), Co (hcp), and Fe (bcc)]. It is at once apparent from Fig. 14 that the optical densities of states of these three materials cannot be related via the rigid-band model. According to that model, the Co and Fe densities of states would be derived from that of Ni simply by moving the Fermi level downward to account for the

³² See the end of Sec. V C for a more detailed discussion of this point.

³³ There seems to be a tendency for peak 3 to decrease in magnitude and to decrease slightly in energy with the decreasing number of d electrons, i.e., as one goes from Ni to Fe.

reduced number of valence electrons/atom; thus any structure in the density of states would move progressively closer to the Fermi level with decreasing atomic number. For example, if one started with the nickel optical density of states and removed two electrons to form iron, the iron Fermi level should be about 2 eV below that of nickel, i.e., the iron Fermi level should fall near peak 2. As can be seen from Fig. 14, this is not the case; rather, the position of the structure (particularly peaks 1 and 2) remains fixed with respect to the Fermi level or moves slightly (peak 3) in the direction *opposite* to that predicted by the rigid-band model. If the optical densities of states are closely related to the ground-state densities of states, this result would indicate that the band structures of Co, Fe, and Ni cannot be related³⁴ via the rigid-band model³⁵; however, if the many-body effects are sufficiently strong so that the optical densities of states are not closely related to the ground-state densities of states, the results could indicate that the many-body or matrix-element effects overwhelm the effects of the ground-state densities of states and produce identical optical densities of states for the three ferromagnetic transition metals.

In view of the similarity between the optical densities of states of Fe, Co, and Ni, it is interesting to make a comparison with Cu and Pd. As noted previously, the optical densities of states of Cu and Ni are not well correlated by the rigid-band model, although Cu does appear^{1,36} to have a deep peak corresponding to peak 3 (Fig. 14). A comparison of the ferromagnetic transition materials with Pd is particularly important, since Pd lies at the end of the second transition-metal series but is not ferromagnetic (Ni lies at the end of the first transition series). As noted earlier, a peak corresponding to peak 3 in Fig. 14 does not occur in Pd, although peaks similar to peaks 1 and 2 do occur.^{4,7,37} This suggests a strong difference between Pd and the ferromagnetic transition metals. This again might be due to a large difference in band structure³⁸ (and thus in the potential seen by the electrons) or to a strong difference in the many-body effects. Note that a correlation exists between the occurrence of peak 3 and the occurrence of ferromagnetism.³⁹ Whether this correlation is meaningful

or accidental can only be determined by additional study.

The optical densities of states can be compared with the densities of states obtained from band calculations.⁴⁰⁻⁴⁵ The densities of states from at least five band calculations for Ni are available. These calculations give d bandwidths between approximately 4.5 and 6.0 eV. Although there is considerable variation in the details of the calculated densities of states, they all have a predominant peak at a few tenths of an eV below the Fermi level (this corresponds to peak 1 in Fig. 14) and quite strong structure 1.4 to 2.6 eV below the Fermi level (corresponding to peak 2 in Fig. 14). For a majority of the calculations, the peak near the Fermi level and the peak or peaks near 2 eV are the most important structures in the density of states. As was noted above, this structure corresponds rather well to the peaks 1 and 2 in Fig. 14. In general, the peaks in the calculated density of states are narrower and sharper than the peaks in Fig. 14; however, this difference could be due to lifetime broadening of the experimental structure.⁴⁶ In a majority of the calculated densities of states, no very strong structure is found 4 to 5 eV below the Fermi level, i.e., no peak corresponding to peak 3 in Fig. 14. There are two exceptions. In the calculations of Hodges, Ehrenreich, and Lang,⁴² taking hybridization into account, distinct structure appears at about $E_f - E \cong 4.0$ eV. The relative height of this peak is about three times lower than of the peak in the optical density of states. This difference might be due to an optical-matrix-element enhancement of the optical density of states. Of considerable interest is the recent band calculation⁴⁴ for Ni which used a $\frac{2}{3}\rho^{1/3}$ exchange potential; this calculation gave considerably increased d bandwidth as well as a peak in the density of states at $E_f - E = 4.5$ eV. This peak is not so large as the peak observed in the optical density of states. There are questions concerning the relationship between the eigenenergies obtained using the $\frac{2}{3}\rho^{1/3}$ exchange and the binding energies (the latter are closely related to the present measurements); however, in view of these continuing developments in band calculations and the uncertainty as to the appropriate potential,⁴⁷ it does not seem possible at present to arrive at any final conclusion as to the relationship between the optical density of states and the results obtained from band theory. The possibility of ultimate agreement between

³⁴ In their band calculation of Ni for various atomic configurations, Snow *et al.* have noted possible difficulties with the rigid-band model. See E. C. Snow, J. T. Waber, and A. C. Switendick, *J. Appl. Phys.* **37**, 1342 (1966).

³⁵ If matrix-element enhancement as described earlier were important, the conclusions concerning the failure of the rigid-band model would still hold.

³⁶ W. F. Krolikowski, Ph.D. dissertation, Stanford University, 1967 (unpublished).

³⁷ In a subsequent publication, the complete photoemission and optical study of Pd will be reported, and a detailed comparison will be made with the ferromagnetic transition metals.

³⁸ If a matrix-element enhancement is important in giving strength to the deep peak in Ni, Co, Fe, and Cu, the absence of this peak in Pd would suggest a detailed change in the character of the wave functions of Pd.

³⁹ The occurrence of the deep peak in Cu suggests that interactions occur in Cu which are similar to those in Ni, Co, and Fe; however, since the Cu d states are completely full, this cannot lead to ferromagnetism.

⁴⁰ J. G. Hanus, Solid State and Molecular Theory Group, MIT Quarterly Progress Report No. 48, 1963, p. 5 (unpublished).

⁴¹ S. Wakoh and J. Yamashita, *J. Phys. Soc. Japan* **19**, 1342 (1964).

⁴² L. Hodges, H. F. Ehrenreich, and N. D. Lang, *Phys. Rev.* **153**, 574 (1966).

⁴³ E. C. Snow, T. J. Waber, and A. C. Switendick, *J. Appl. Phys.* **37**, 1342 (1966); and (private communication).

⁴⁴ J. W. D. Connolly, *Phys. Rev.* **159**, 415 (1967).

⁴⁵ E. D. Thompson and J. Meyers, *Phys. Rev.* **153**, 574 (1967).

⁴⁶ Note that neither soft x-ray spectroscopy (SXS) nor ion-neutralization spectroscopy (INS) has resolved more than a single peak in the Ni valence-band density of states.

band calculation and the optical density of states, however, cannot be ruled out.

Densities of states for Ni and Cu obtained by ion-neutralization spectroscopy (INS)⁴⁸ and from x-ray-emission spectra (SXS)^{30,49-51} have been reported. These have been compared to the results obtained from photoemission and optical studies (PES).^{30,51} In general, INS and SXS resolve only a single peak for the *d* states. In most cases, the total *d* width is found to be less in SXS and INS than in PES. No evidence is reported for the peak 4.5 eV below the Fermi level in INS. A rather weak shoulder is evident at 4.5 eV in the SXS data of Cuthill *et al.*^{30,51} The difference between the results obtained using PES, INS, and SXS suggests, at least to the present authors, that one must be cautious at present in claiming that the results of any one of these methods give directly the densities of states of the unperturbed materials.

With regard to possible matrix-element effects, we should note band calculations by Stern,⁵² Wood,⁵³ and Ingalls⁵⁴ for Fe, which indicate that the nature of the *d* states changes with energy as one goes through the *d* band. As Cuthill *et al.*³⁰ have pointed out, this could lead to a strong energy dependence of matrix elements, which might explain the deep peak seen in Cu, Ni, Co, and Fe. In particular, Stern and Wood find that *d* states near the bottom of the *d* bands tend to have a more diffuse charge distribution than do states near the top of the bands. For example, Wood found that uppermost *d* states had less spatial extent in the solid than in the atom (i.e., have an antibonding nature), whereas the lowest *d* states were much less spatially confined than the atomic *d* states (bonding states). Stern calculates a large cohesive energy using these wave functions. Cuthill *et al.* estimate that the optical matrix element for transitions from the lowest *d* states will be about a factor of 10 larger than that from the uppermost states. This could account for the strong deep peak in the optical density of states, without necessitating the placing of a large peak in the unperturbed density of states at this point. The systematics of the deep peak in a different material would then be correlated with the existence and location of the "bonding states," e.g., their absence in Pd would indicate the absence of bonding states. However, the INS data of Hagstrum⁴⁸ may

⁴⁷ In addition to the uncertainty in the exchange potential, a certain amount of uncertainty may be present in determining the appropriate starting charge distribution which should be used to determine the potential if completely unambiguous, self-consistent calculations are not made. This has been particularly well pointed out by the work of Snow *et al.*

⁴⁸ H. D. Hagstrum, *Phys. Rev.* **150**, 495 (1966).

⁴⁹ J. Clift, C. Curry, and B. J. Thompson, *Phil. Mag.* **8**, 593 (1963).

⁵⁰ Y. Cauchois and C. Bonnelle, *Optical Properties and Electronic Structure of Metals and Alloys* (North-Holland Publishing Co., Amsterdam, 1966), p. 83.

⁵¹ J. R. Cuthill, A. J. McAlister, and M. L. Williams, *Phys. Rev. Letters* **16**, 993 (1966).

⁵² F. Stern, *Phys. Rev.* **116**, 1399 (1958).

⁵³ J. H. Wood, *Phys. Rev.* **117**, 714 (1960).

⁵⁴ R. Ingalls, *Phys. Rev.* **155**, 157 (1967).

argue against the existence of "bonding states." The tunneling probability, which is so important in the INS experiment, depends strongly on the radial extent of the wave functions. If the wave functions were highly confined for states near the top of the *d* band and more diffuse for states at the bottom of the band, one would expect a peak in the density of states obtained from INS corresponding to the bottom of the *d* band, unless the tunneling probability decreases sufficiently with decreasing energy. This is not observed. Rather, the *d*-band density of states obtained from INS peaks strongly near the top of the *d* band and seems to approach zero at the bottom of the band. In view of the changes in band calculations since 1962, it is probably necessary for a much more systematic investigation of the calculated wave functions and matrix elements to be made before their importance can be completely evaluated.

We have mentioned the possibility that the optical density of states would differ from the density of states calculated on the basis of band theory because of many-body effects. If this is the case, the optical density of states could provide a powerful tool in studying the many-body interactions. It is possible that the deep peak (peak 3 in Fig. 14) seen in photoemission is a reflection of these many-body interactions. There is the possibility that many-body effects might be important in ferromagnetism. In the next few paragraphs, we will discuss briefly some of the relevant theoretical suggestions made to date.

Phillips⁵⁵ has suggested that the enhanced cohesive energy of the noble and transition metals may be due to a many-body resonance and that the deep peak (peak 3 in Fig. 14) in the optical density of states of the transition metals is due to this resonance. Using this approach and the available optical data, Phillips has made predictions of deep peaks in the optical density of states which have since found some verification in photoemission and optical studies.^{7,36}

Mott⁵⁶ has noted that, if Van der Waal's interactions are important to the cohesive energy, excitation of material in the virtual state produced by those interactions is possible and could produce a deep peak in the optical density of states. He has also pointed out⁵⁷ that Ni metal may contain atoms which instantaneously have the d^8 configuration and that a deep peak might result from the excitation of an atom in such a state. Since atomic nickel has the configuration $3d^84s^2$, whereas Pd has the configuration $4d^{10}$, Ni would be much more likely to have the d^8 configuration than Pd. This correlates with our finding the deep peak in Ni and not in Pd. Mott has pointed out that, if the d^8 state did exist in Ni, it could lead to ferromagnetism.

⁵⁵ J. C. Phillips, *Phys. Rev.* **140**, A1254 (1965).

⁵⁶ N. F. Mott (private communication).

⁵⁷ N. F. Mott, *Advan. Phys.* **13**, 325 (1965). See also the comments at the end of Ref. 1 therein.

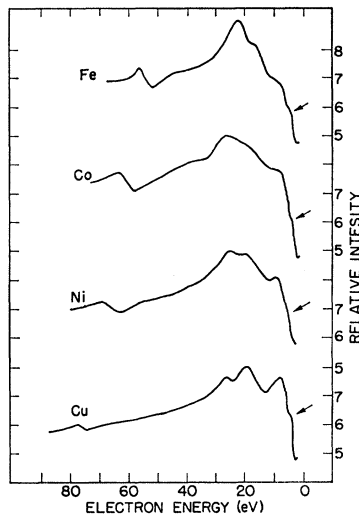


FIG. 15. Characteristic energy loss for the transition metals from Robins and Swain (Ref. 21).

Nesbet and Grant⁵⁸ had recently examined the occurrence of nondirect transitions in terms of second-order (or higher-order) processes in which the nondirect electronic excitations are coupled in the excitation process to secondary excitations that make up the necessary \vec{k} . They attribute the nondirect character of the transitions seen in many metals for photon energy less than the plasma energy to a combination of phonon indirect processes and of secondary excitation of low-energy electron-hole pairs. It is very important to note that the secondary excitation takes place simultaneously with the nondirect transition and is not a scattering event subsequent to the nondirect excitation process. Nesbet and Grant further point out that the production of a collective excitation simultaneously with the nondirect would open an additional "channel" for the nondirect process; however, in this case, the single electrons excited via the nondirect process would be reduced in energy by an amount equal to the energy of the collective oscillation. Thus they suggest that the peak near -5 eV in the optical density of states of Ni, Co, and Fe is due to such a collective excitation; further, they find correlation between the position of this peak and the first (rather weak) structure in the characteristic energy-loss spectra²¹ (see Fig. 15). If the suggestion of Nesbet and Grant does provide the correct explanation for the deep peak, the question rises at once as to why a collective oscillation occurs at about 5 eV in the ferromagnetic transition metals and only at higher energies in Pd.³⁷ One might also ask about the detailed origin of these rather low-energy collective oscillations.

Cuthill *et al.*⁵¹ have also suggested that the deep peak in the Ni optical density of states is due to the simultaneous excitation of two electrons by a single photon

⁵⁸ R. K. Nesbet and P. M. Grant, Phys. Rev. Letters **19**, 222 (1967).

and that because of this, all of the optical and photo-emission data can be explained in the framework of optical transitions where \mathbf{k} is an important optical selection rule. We find serious difficulties with this suggestion. A detailed analysis is given in Appendix B of this paper.

ACKNOWLEDGMENTS

The authors would like to acknowledge useful discussions with Dr. Frank Herman, Dr. Arthur Freeman, Dr. Robert Nesbet, Dr. J. C. Phillips, Sir Nevill Mott, Dr. Edward Snow, Dr. Karvel Thornber, and Dr. John Wood. They are also grateful to Dr. J. R. Cuthill, Dr. A. J. McAlister, Dr. M. L. Williams, and Dr. R. E. Watson for a preprint of their paper and for useful discussions.

APPENDIX A: ESTIMATES OF THE ELECTRON-ESCAPE LENGTH $L(E)$

$P(E)$ has been determined from experimental EDC's as described in Sec. III and is shown in Fig. 10. If $T(E)$ were known, $L(E)$ could be calculated using Eq. (2):

$$L(E) = \frac{1}{\alpha N_c(E) T(E) - P(E)} P(E) \quad (\text{A1})$$

If $L(E)$ were known, $T(E)$ could be similarly calculated. Unfortunately, neither $T(E)$ nor $L(E)$ is known experimentally for Co. We wish to gain whatever information possible about $L(E)$ from photoemission data because of considerable current interest about hot-electron transport in metals.⁵⁹

A simple form of $T(E)$ will be assumed for this purpose—the free-electron threshold function¹⁴

$$T(E) = \begin{cases} \frac{1}{2} \{ 1 - [(\varphi - E_B)/(E - E_B)]^{1/2} \}, & \text{if } E \geq \varphi \\ 0, & \text{if } E < \varphi. \end{cases} \quad (\text{A2})$$

The Fermi level is taken to be the zero of energy. In this equation, E_B is an adjustable parameter. Two limiting values were chosen. In one case, it is placed just above the high density of states in the conduction band, $E_B - E_f = 2$ eV. In the second case, it is placed just below the vacuum level, $E_B - E_f = 4.4$ eV. The two resultant [from Eq. (A1)] $L(E)$ curves corresponding to the two E_B values are shown in Fig. 16. These two curves probably are the limiting cases. Also shown in Fig. 16 are two calculated curves which give the shape of $L(E)$ based on two models; it must be emphasized that since the calculations did not include a calculation of matrix elements, *there is no significance* to the magnitude of the calculated escape $l_e(E)$ —only the shapes are significant. The dotted curve shows the results obtained^{7,14,36} using the deduced optical density

⁵⁹ S. M. Sze, C. R. Crowell, G. P. Carey, and E. E. LaBate, J. Appl. Phys. **37**, 2690 (1966); S. M. Sze, J. L. Moll, and T. Sugano, Solid-State Electron. **7**, 509 (1964).

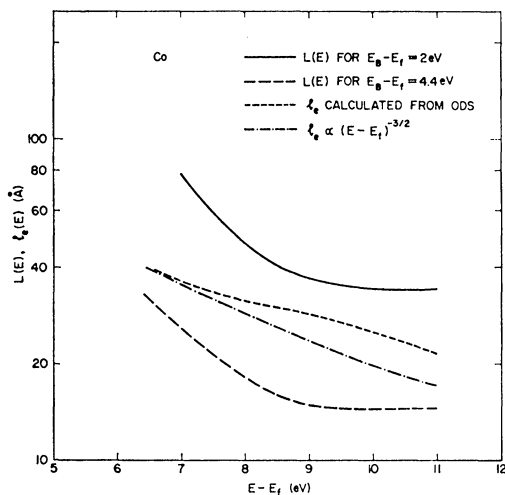


FIG. 16. Comparison of experimental $L(E)$ and calculated $l_e(E)$.

of states and assuming a free-electron group velocity. The dash-dot curve is a simple analytic form based on the free-electron model.^{36,60} The magnitudes of these calculated curves have been adjusted to make them lie between the two $L(E)$ curves. The calculated curves decrease more slowly than the measured curves for $E - E_f \leq 9$ eV but faster than the measured curves for $E - E_f \gtrsim 9$ eV.

In contrast to the rather poor agreement between the shape of the $l_e(E)$ and measured $L(E)$ for Co, very good agreement has been found for the noble metals.³⁶ This is probably because in the noble metals, the d states lie much farther from the vacuum level than in Co. Therefore the free-electron approximation for the group velocity is much better for the noble metals than for Co. Thus the $T(E)$ that we assumed probably is not a good approximation for Co. Consequently the deduced $L(E)$ is uncertain. Another point is that in the calculation of l_e from the optical density of states, it is assumed that the matrix element of electron-electron scattering is a constant. This may not be justified for Co.

APPENDIX B: COMMENT ON THE TWO-ELECTRON MODEL OF CUTHILL, McALISTER, AND WILLIAMS

Cuthill, McAlister, and Williams (CMW) have suggested that the deep peak observed in Ni (peak 3 in Fig. 14) is due to one of the two electrons being excited from the same initial energy by a single photon.⁵¹ According to their model, one of the two transitions would correspond to a "very strong" direct interband transition, and thus the final-state energy E_1 (as well as the energy of the initial state) would be independent of $h\nu$. The second electron of the excitation pair would be excited from a state with the same initial energy as the first and would carry off the excess energy, so that

⁶⁰ A. Ross, RCA Rev. 27, 600 (1966).

its final energy in vacuum E_2 would be given by

$$E_2 = h\nu - E_{ib} - \delta - \varphi. \quad (B1)$$

Here, E_{ib} is the energy of the strong interband transition, δ is the energy of the initial state with respect to the Fermi energy (δ is positive), and φ is the work function of the metal. CMW also state that their model "has the further advantage of working within the framework of conventional band theory with \mathbf{k} -conserving transitions." The last statement cannot be true in general. For it to be true, both transitions would have to be direct, and both would originate from a single initial-state energy. However, since E_2 , the final-state energy of the second electron, must change continuously with energy as $h\nu$ changes [see Eq. (B1)], and since, in general, there will not be a continuous range of final energy states for direct transitions originating from a fixed initial energy, the model of CMW *does not* work within the framework of conventional band theory with \mathbf{k} -conserving transitions. It would only work within that framework if the initial band were completely flat, i.e., if all values of \mathbf{k} were degenerate at the same value of energy. As has been pointed out previously,^{1,61} the distinction between direct and nondirect transitions loses meaning when this is the case.

On the basis of their model, CMW went to the literature and made assignments for the strong direct transition E_{ib} , as well as for δ , E_1 , and E_2 . They achieved considerable apparent success in finding peaks which agreed with their model; however, as will be illustrated in detail below, this was due in large part to the liberty taken with the available data.

An extreme example of this occurred in their choice of the "very strong interband" transition for Ag. Figure 17 gives the ϵ_2 curve for Ag from the source⁶² referred to by CMW.⁶³ CMW stated that a "very strong" interband transition occurs at 6.4 ± 0.5 eV. As can be seen from Fig. 17, there is no distinguishable peak at that photon energy (marked by arrow 1 in the figure). CMW ignored the only strong peak in ϵ_2 , that at 4.0 eV. They also stated that characteristic energy-loss studies showed a strong transition at 6.4 ± 0.5 eV. Again no

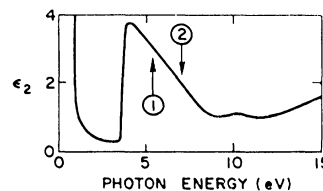


FIG. 17. ϵ_2 of Ag (Ref. 61).

⁶¹ H. Ehrenreich, *Optical Properties and Electronic Structure of Metals and Alloys* (North-Holland Publishing Co., Amsterdam, 1966), p. 110. See, in particular, the comment by W. E. Spicer at the end of that article.

⁶² H. Ehrenreich and H. R. Philipp, Phys. Rev. 128, 1622 (1962).

⁶³ CMW referred to the optical conductivity $\sigma = \omega \epsilon_2$. No curve of σ is given in the work referred to by CMW; rather, the ϵ_2 curve shown in Fig. 17 is given. The remarks made here, however, are not affected by this.

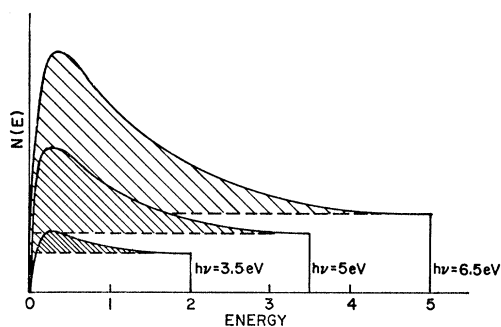


FIG. 18. Theoretical EDC's for a metal, including the effect of electron-electron scattering. The cross-hatched area indicates the contribution due to once-scattered electrons.

such evidence exists, although such transitions⁶⁴ do occur at 4.0 and 7.5 eV. Subsequent to their original paper, CMW have stated³⁰ that an error was made in interpreting the optical data and that the very strong optical transition lies at 7.5 or 8.0 eV (indicated by arrow 2 in Fig. 17). As can be seen from Fig. 17, there is no noticeable structure in ϵ_2 , which occurs at 7.5 or 8.0 eV. The 7.5-eV figure agrees with a characteristic energy loss; however, examination of ϵ_1 and ϵ_2 indicates that the rather broad energy-loss peak is associated with a maximum in $\epsilon_2/(\epsilon_1^2 + \epsilon_2^2)$ because of the combined effect of an ϵ_1 , which is increased from a low value with increasing $h\nu$, and an ϵ_2 , which is decreased from a high value. It is clearly not due to strong structure in ϵ_2 at 7.5 or 8.0 eV. As will be shown later, if 7.5 or 8.0 eV is used for the direct transition, difficulties must arise with other assignments⁶¹ of CMW. In Cu, strong peaks appear⁶² in σ or ϵ_2 near 2.3 and 4.7 eV. The 4.7-eV peak was used in the CMW model, but the 2.3-eV peak was ignored.

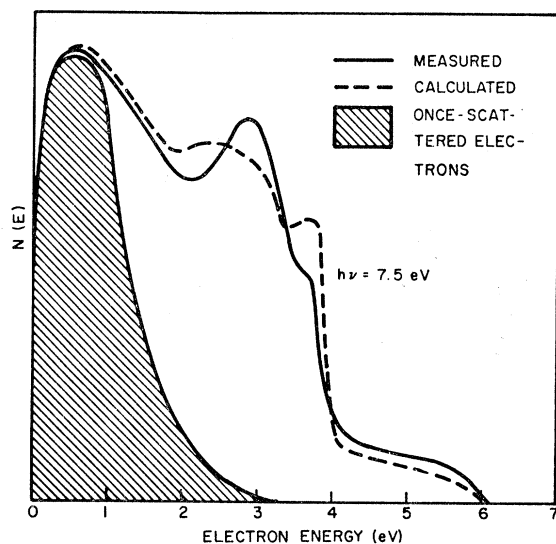


FIG. 19. Calculated and measured EDC's, $h\nu = 7.5$ eV.

⁶⁴ J. L. Robins, Proc. Phys. Soc. (London) 78, 1177 (1961).

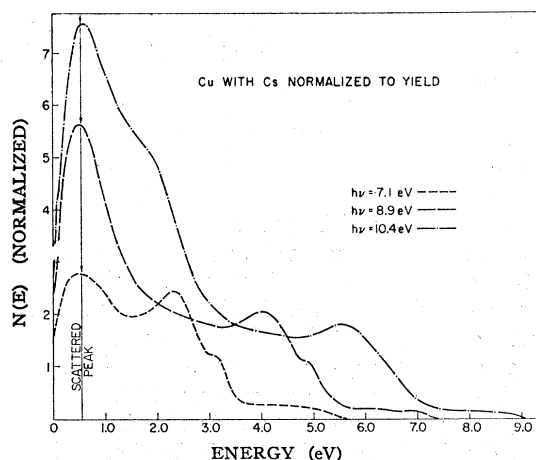


FIG. 20. EDC's of Cu with a monolayer of Cs.

CMW expected two peaks in the photoemission-energy-distribution curves due to the two-electron event. The first, due to the strong direct transition, would be at E_1 and would be independent of $h\nu$; the second, which moves with $h\nu$, would occur at an energy given by Eq. (B1). E_1 was located at about 0.5 eV above the vacuum level in cesiated Cu and Ag (based on their original model for Ag) and below the vacuum level, making it impossible to observe in Ni. A peak near 0.5 eV is observed in Cu and Ag; however, this peak has very detailed characteristics and has been shown to be due to the electrons produced by conventional electron-electron scattering of the primary photo-excited electrons. The internal distribution due to this process is ramp-shaped, with the maximum near the Fermi surface and the number of scattered electrons decreasing monotonically with energy.¹⁴ The high-energy cutoff of the distribution is determined by the photon energy. To obtain the external energy distribution, one must multiply the internal distribution by the function giving the escape probability of the electrons

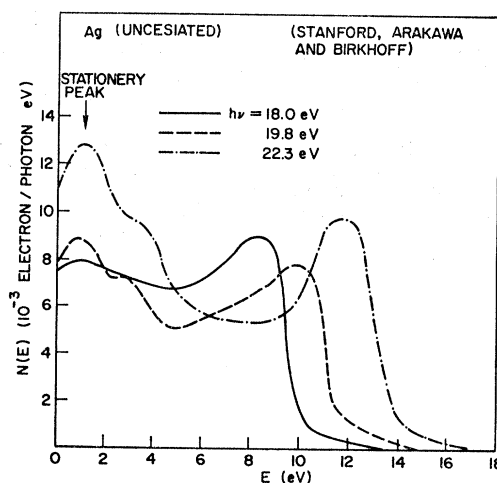


FIG. 21. EDC's of Ag at $h\nu = 18.0, 19.8,$ and 22.3 eV, plotted versus E .

$T(E)$. This function is zero for energy below the vacuum level and rises rather sharply above the energy.¹⁴ As has been shown previously,¹⁴ the external distribution due to the "conventional" scattered electrons will be given by the product of the decreasing ramp function and the increasing escape function. Because of the sharp increase in the escape function just above the threshold, a peak will be produced in the distribution just above the vacuum level, i.e., at about 0.5 eV. In Fig. 18, we present external distributions of the scattered electrons calculated¹⁴ for a simple case. Note that the position of the peak (which is determined principally by the vacuum level) does not move with $h\nu$ and that the height of the peak grows monotonically with $h\nu$. In Fig. 19, we present data¹⁴ for Cu, showing an experimental distribution as well as a calculated curve including the contribution of the scattered electrons. As can be seen from that figure, the scattered electrons provide the peak near 0.5 eV. As Fig. 18 shows, this peak should be stationary but should increase in magnitude with increasing $h\nu$. Figure 20 shows¹ that this is indeed the case.⁶⁵ Note that, except for the structure imposed by the unscattered electrons, the shape of the experimentally scattered distribution in Figs. 18 and 19 is in agreement with the theoretical calculations. For further details, the reader is referred to published articles.^{1,14} CMW have given no reason why the height of the low-energy peak should increase monotonically with $h\nu$, as observed experimentally. It should be emphasized that the position of the peak is just set by the value of the work function and will only appear when the photon energy is several times the work function.

CMW made two predictions for uncesiated Ag based on their model. The first was that no low-energy peak would appear for large values of $h\nu$. (However, one should appear for sufficiently large $h\nu$ if the low-energy peak is due to conventional scattering as described above.) In Fig. 21, we present high-photon-energy data of Stanford, Arakawa, and Birkhoff.⁶⁶ Note that a stationary low-energy peak appears and grows with increasing $h\nu$. This result confirms the predictions of the conventional scattering model and contradicts the

⁶⁵ The curves in Fig. 20 have been normalized to yield so that the height of each peak is proportional to the number of electrons emitted with the indicated energy.

⁶⁶ J. L. Stanford, E. T. Arakawa, and R. D. Birkhoff, Oak Ridge National Laboratory Report No. ORNL-TM-1392, 1966 (unpublished).

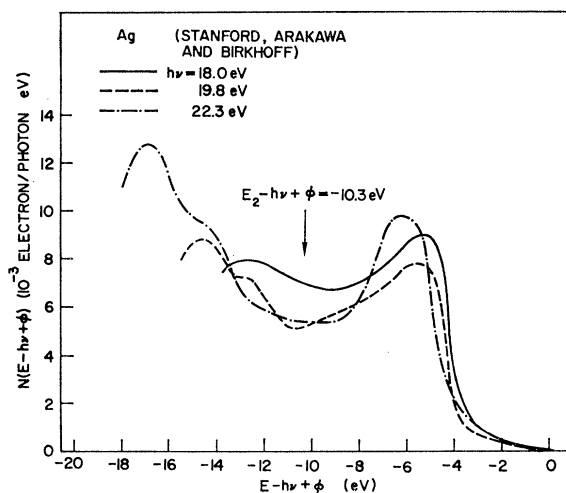


FIG. 22. EDC's of Ag at $h\nu=18.0, 19.8,$ and 22.3 eV, plotted versus $E-h\nu+\phi$.

model of CMW. Thus all evidence points to the fact that the low-energy stationary peak is due to conventional scattering and not to the two-electron effect predicted by CMW.

In their original paper, CMW predicted that in Ag peak E_2 should appear at about 10.3 eV below the Einstein limit. In Fig. 22, we present the data of Stanford *et al.* shifted so that the Einstein limits coincide. There is no peak at -10.3 eV as predicted by the CMW model. On the basis of their reassignment of the very strong interband transition, CMW now predict a peak 7.5 or 8.0 eV below the maximum energy, in agreement with the peak seen by Stanford *et al.* near -12.0 eV in Fig. 22. However, if this value is used for the very-strong-interband-transition peak E_{ib} in cesiated Ag, the position of E_1 would be changed. If the initial state remains the same, E_1 would be expected at about 3 eV instead of 0.5 eV, as given in their paper.⁵¹ There is no stationary peak in the experimental distribution at 3.0 eV.

As shown above, the two original predictions made by CMW were found to be incorrect by the experiments of Stanford *et al.* There are also a number of very serious questions concerning the choice of experimental data which CMW used to support their model. In view of this, it appears that the detailed model set forth by CMW to explain the difference between the SXS, INS, and PES data should be discarded.